Supplementary Materials for

Countering Zika in Latin America

Neil M. Ferguson,* Zulma M. Cucunubá, Ilaria Dorigatti, Gemma L. Nedjati-Gilani, Christl A. Donnelly, Maria-Gloria Basáñez, Pierre Nouvellet, Justin Lessler

*Corresponding author. E-mail: neil.ferguson@imperial.ac.uk

Published 14 July 2016 on *Science* Express
DOI: 10.1126/science.aag0219

This PDF file includes

Other Supplementary Materials for this manuscript include the following:
(available at www.sciencemag.org/cgi/content/full/science.aag0219/DC1)

Data files S1 to S45 as a zipped archive:
- Reported weekly Zika cases by country and for Brazilian regions (36 comma-separated value [CSV] files)
- Sources for country data (1 CSV file)
- Time windows for estimation of reproduction number used by R code (2 CSV files)
  (used to calculate *R*, the reproduction number)
- *R* estimates for Brazil and Latin America (2 CSV files)
- Code used for estimation of reproduction number, *R* (2 R files)
- Zika spatial simulation code (1 Berkeley Madonna MMD file)
- Readme file (1 text file)

Contents

Materials and Methods

1. Case data and sources

1.1 Zika Cases

Based on the weekly Zika reports by the Pan American Health Organization (PAHO) (*12*), the number of weekly suspected and confirmed cases and the estimated cumulative incidence have been obtained from the 35 countries/territories in the Americas that have reported cases (Table S1). We use the term 'confirmed cases' to mean those with laboratory confirmation and 'suspect cases' to denote cases that have been clinically diagnosed (variously called 'suspect' or 'clinically confirmed') without laboratory confirmation.

Original sources for weekly data by country have been obtained from the weekly case reports on the PAHO website (*13*). For some countries, data have been double checked from national weekly reports or other sources detailed below:

- **Colombia:** weekly reports of suspected and confirmed cases (*14*)
- **México:** weekly official reports refer only to confirmed cases (*15*).
- **Dominican Republic:** weekly epidemiological reports on suspected and confirmed cases (*16*).
- **El Salvador:** weekly epidemiological reports on suspected and confirmed cases (*17*)
- **Panamá:** weekly epidemiological reports on suspected and confirmed cases (*18*)
- **Honduras:** weekly epidemiological reports on suspected and confirmed cases (*19*)
- **Brazil**: started mandatory Zika case notification on 17th February 2016. There is no official information at the national level for 2015. Only two official reports have been released with information of cumulative cases for 2016:

  As of week 13 : total number of 91,387cases (*20*)

  As of week 16 : total number of 120,161 cases (*21*)

  To obtaining weekly information we have used officially released data from 10 states, as shown in Table S2. Over the 10 states there are a total of 176,351 reported suspected Zika cases, (85,117 in 2015 and 91,234 in 2016), which corresponds to ~ 76% of the informed cumulative data at the national level for 2016.

When data was only in graphical forms, the WebDigitizer tool (http://arohatgi.info/WebPlotDigitizer/app/) was used to extract the approximate number of reported cases.

For reference, we provide the data we collated on Zika case incidence in CSV file format.

Table S1. Cumulative Zika suspected and confirmed cases reported to PAHO by country and territory in the Americas, 2015-2016. Updated as of 02 June 2016. Population sizes taken from reference (*22*).

Country / territory	Suspect Zika	Confirmed Zika	Total Zika	Population	Cumulative Incidence*100k
Argentina	1,613	19	1,632	40,117,096	4.1
Aruba	-	17	17	110,000	15.5
Barbados	316	7	323	283,000	114.1
Belize	-	2	2	369,000	0.5
Bolivia	99	11	110	10,520,000	1.0
Brazil *	154,270	39,993	194,263	204,519,000	95.0
Colombia	80,953	6,402	87,355	48,218,000	181.2
Costa Rica	2,090	58	2,148	4,851,000	44.3
Cuba	-	1	1	11,252,000	0.0
Curacao	-	73	73	157,000	46.5
Dominica	203	28	231	71,000	325.4
Dominican Republic	2,370	73	2,443	9,980,000	24.5
Ecuador	393	143	536	16,279,000	3.3
El Salvador	11,631	46	11,677	6,460,000	180.8
French Guiana	6,700	483	7,183	262,000	2,741.6
Guadeloupe	6,320	379	6,699	405,000	1,654.1
Guatemala	1,089	1,162	2,251	16,176,000	13.9
Guyana	-	6	6	747,000	0.8
Haiti	1,777	5	1,782	10,994,000	16.2
Honduras	21,025	44	21,069	8,950,000	235.4
Jamaica	646	14	660	2,729,000	24.2
Martinique	26,650	12	26,662	383,000	6,961.4
Mexico	-	314	314	121,006,000	0.3
Nicaragua	-	207	207	6,514,000	3.2
Panamá	638	274	912	3,764,000	24.2
Paraguay	273	8	281	7,003,000	4.0
Peru	-	5	5	31,760,204	0.0
Puerto Rico	10,535	1,170	11,705	3,508,000	333.7
Saint Barthelemy	19	7	26	9,036	287.7
Saint Lucia	-	2	2	172,000	1.2
Saint Martin	425	109	534	36,000	1,483.3
Saint Vincent and the Grenadines	-	2	2	110,000	1.8
Sint Maarten ¥	-	7	7	39,000	17.9
Suriname	2,503	527	3,030	560,000	541.1
Trinidad and Tobago	-	16	16	1,357,000	1.2
Virgin Islands	228	21	249	105,000	237.1
Venezuela	31,224	352	31,576	30,620,000	103.1
Total	**363,990**	**51,999**	**415,989**	**600,395,336**	69.3

** For Brazil these are only cases for 2016. Additionally, their 39,993 confirmed cases include laboratory and clinically confirmed cases.*

¥French side of Saint Martin

Table S2. Cumulative Zika suspected and confirmed cases reported at the subnational level in Brazil, 2015-2016. Updated as of 09 June 2016. Population sizes taken from reference (*23*)

Region	State or City	Cases 2015	Cases 2016*	Cumulative cases	Cumulative Incidence *100k	Information up to	Population	Source
North	Acre	42	746	788	99.7	09/04/2016	803,513	(*24*)
Northeast	Bahía	66,543	46,314	112,857	746.1	21/05/2016	15,203,934	(*25*)
	Pernambuco	2,816	8,338	11,154	120.2	21/05/2016	9,345,173	(*26*)
Southeast	Espírito Santo	-	1,983	1,983	51.0	02/04/2016	3,929,911	(*27*)
	Rio de Janeiro	6,686	18,845	25,531	155.1	03/04/2016	16,550,024	(*28*)
	São Paulo	-	935	935	42.1	31/03/016	44,396,484	(*29*)
South	Paraná	30	3,824	3,854	34.8	21/05/2016	11,163,018	(*30*)
	Rio Grande do Sul	24	505	529	4.7	21/05/2016	11,247,972	(*31*)
Central-West	Goiânia City	47	2,081	2,128	32.6	30/04/2016	6,610,681	(*32*)
	Mato Grosso	8,929	7,663	16,592	514.6	05/03/2016	3,265,486	(*33*)
Total (10 states)		**85,117**	**91,234**	**176,351**				

** As reported until the last date of information and revised on 9th June 2016*

1.2 Guillain-Barré Syndrome (GBS) in Latin America

As of June 9th 1016, GBS cases confirmed with Zika virus infection and coincident with the Zika epidemic have been reported in 9 countries: Brazil, Colombia, Dominican Republic, El Salvador, French Guiana, Honduras, Martinique, Suriname and Venezuela (*34*)

Weekly information available for four countries is presented in Fig. S1. For Colombia, GBS cases were taken from the PAHO report as of 14 April 2016 (*35*). For El Salvador and Honduras, GBS cases were obtained from the PAHO reports as of 21 April (*36*). For Dominican Republic from the PAHO reports as of 09 June 2016 (*34*)

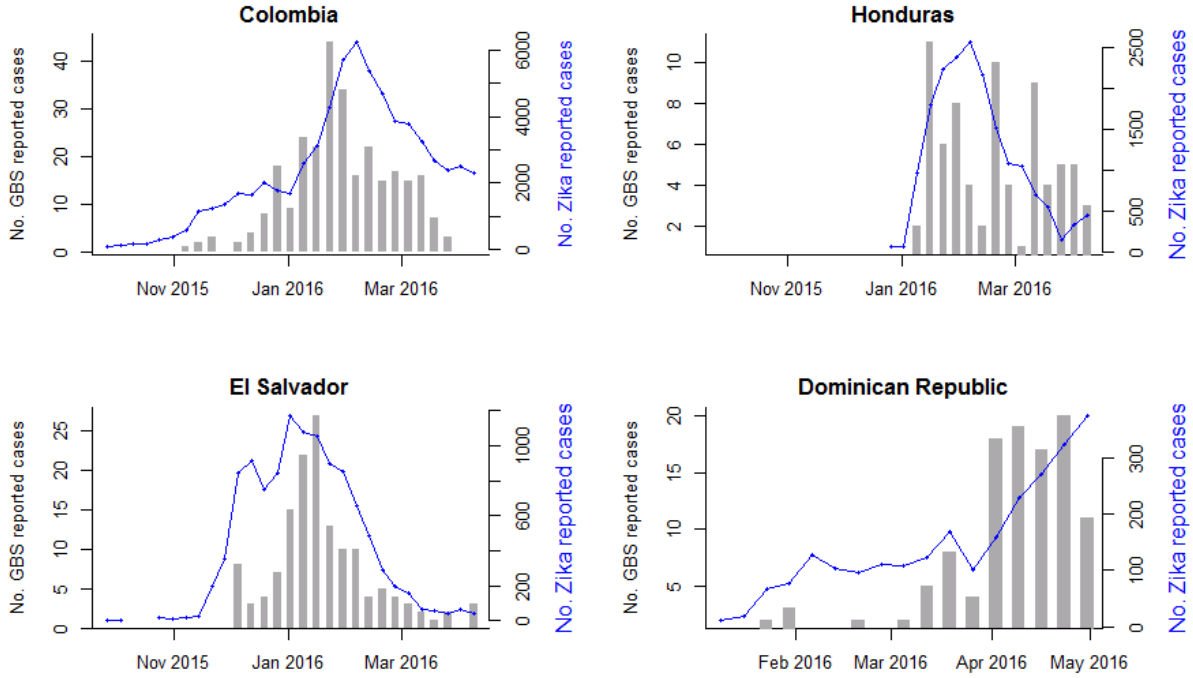

Fig. S1. Guillain-Barré Syndrome cases reported in Colombia, Honduras, El Salvador and Dominican Republic (grey bars, left axis) together with reported suspected Zika cases (blue curves, right axis).

1.3 Microcephaly in Latin America

As of June 9th 1016, confirmed Microcephaly cases coincident with the Zika epidemic have been reported in six countries: Brazil, Colombia, Martinique, Panama, Puerto Rico, and United States (*34*) . Interestingly, in Colombia up to April 2016, the only four microcephaly cases confirmed with Zika infection have been born to asymptomatic women (*37*). As the only country that has reported microcephaly cases in important numbers to be analysed is Brazil, we have plotted the information available for three out of the 10 states that have information for Zika and microcephaly from 2015 simultaneously (Fig. S2).

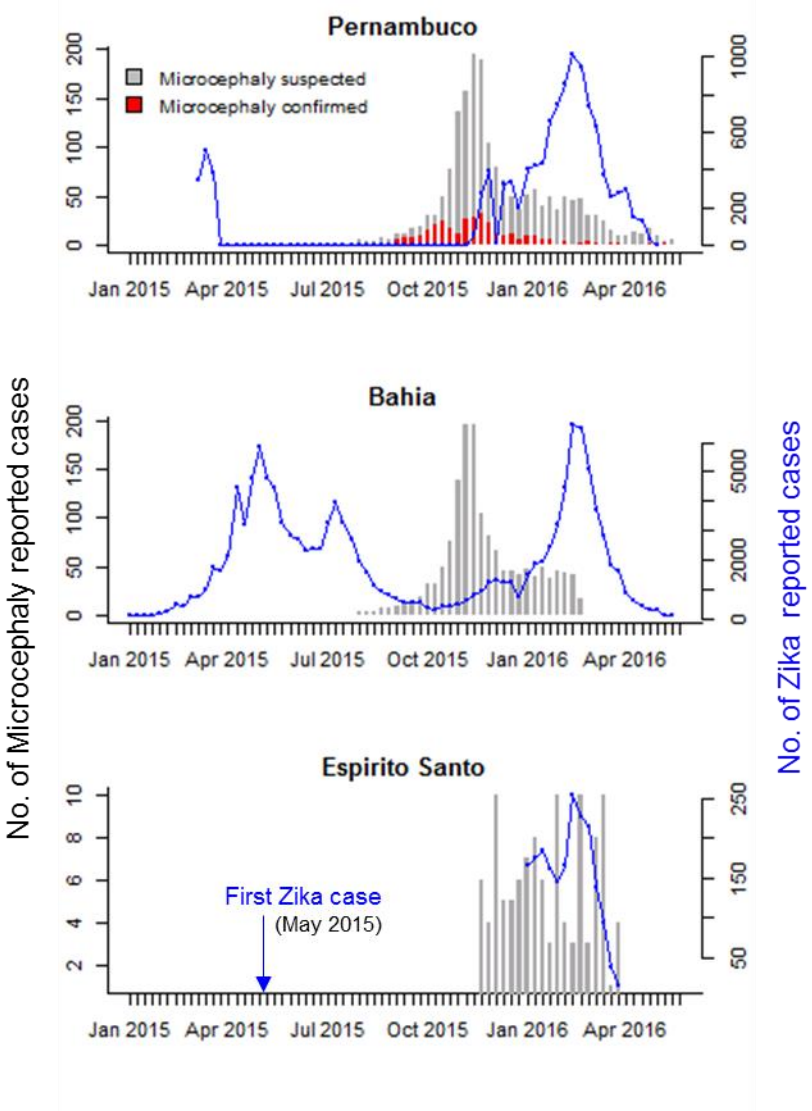

Fig. S2. Microcephaly cases (by week of birth) reported in Pernambuco, Bahia, and Espiritu Santo (grey bars, left axis) together with reported suspected Zika case numbers for those states (blue curves, right axis). For Espiritu Santo there is no detailed data currently available on Zika incidence in 2015 but there is information that the first case was detected in May 2015. In addition, the microcephaly cases for that state may also include other congenital syndromes. For the other two states, a 6-8 month gap is seen between the peak of Zika incidence in 2015 and that of microcephaly incidence.

1.4 Policies on recommending delaying pregnancy

Five countries have recommended that women living in areas at risk of Zika virus infection delay pregnancy (Table S3). In Brazil, officials have publically recommended delay, although it is not an official policy (*4*). Nevertheless, on 7th June 2016, the WHO has extended this recommendation to all countries where autochthonous transmission has been documented (*38*).

Table S3. Latin American countries that have declared delaying pregnancy as a strategy to prevent microcephaly during the Zika epidemic.

Country	Started	Proposed end date	Source reference
Jamaica	18-Jan-2016	31-Dec-2016	(*39*)
El Salvador	20-Jan-2016	01-Jan-2018	(*40*)
Ecuador	20-Jan-2016	Not clear	(*4*)
Dominican Republic	20-Jan-2016	31-Dec-2016	(*41*)
Colombia	07-Jan-2016	01-Jul-2016	(*42*)

2. Natural history parameter estimates

2.1 Viral load data

Using Web of Science, we identified 6 papers (*43-48*) (as of 3 June 2016) reporting the absolute quantification of Zika RNA viral copies in plasma after the onset of symptoms (Figure S3). Additional viral load measurements, which were reported in relative terms (cycle threshold values) in (*49*), were kindly provided by Dupont-Rouzeyrol (personal communication).

Zika viral titers appear to be approximately 2 log10 lower than dengue viral titers (*50*). With the exception of one data point (viral load = 5.5 at day 11 post symptoms onset) and considering the higher lower limits of detection of the assays used in (*50, 51*), the duration of detectable viraemia in the blood appears to be comparable to dengue.

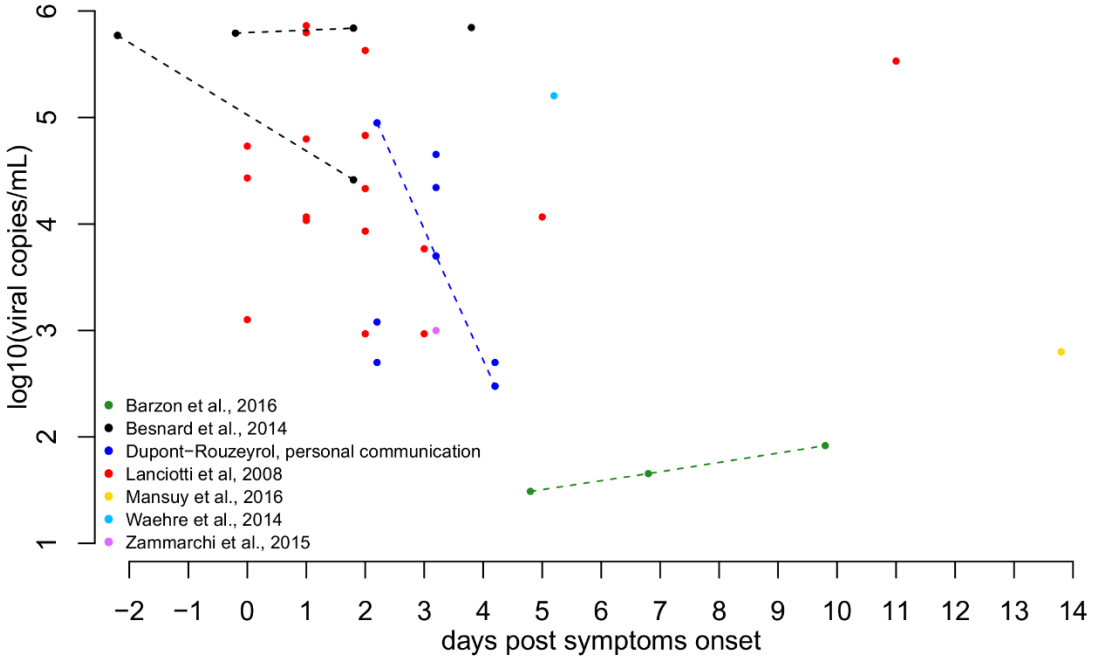

Fig. S3. Viral load detected in plasma in Zika infected cases per day post symptoms onset, by source (*43-48*). Sequential measurements from the same patient have been linked with dashed lines.

2.2 Human-to-mosquito generation time

We derive the human-to-mosquito generation time (*i.e.* the time between human infection and a mosquito taking an infectious blood meal) of Zika virus using information on the distributions of the intrinsic incubation period (IIP) (*i.e.* the time between human infection and symptoms onset) published in reference (*52*) and on the time from symptoms onset to viral clearance ('time to viral clearance'), which we estimated using the same data sources used in reference (*52*).

We denote μ_{IP} and σ_{IP} the mean and standard deviation of the IIP respectively and μ_C and σ_C the mean and standard deviation of the time to viral clearance distribution respectively.

We assume that the time to viral clearance is Gamma distributed with shape parameter α_C and scale parameter β_C, so that the cumulative probability that the time from symptoms onset to viral clearance is ended by day t is

$$F(t;\alpha_C,\beta_C) = \frac{1}{\Gamma(\alpha_C)}\int_0^{t/\beta_C} s^{\alpha_C-1}e^{-s}ds$$

where $\Gamma(\alpha_C)$ is the Gamma function evaluated at α_C.

For each Zika case included in the analysis ($i = 1, \ldots, N$), we denote t_{Pi} the time from symptoms onset to the latest positive sample and t_{Ni} the time from symptoms onset to the first negative sample. The log-likelihood can be written as

$$\mathcal{L}(\alpha_C,\beta_C) = \sum_{i=1}^{N} \ln\big(F(t_{Ni};\alpha_C,\beta_C)\big) - \ln\big(F(t_{Pi};\alpha_C,\beta_C)\big)$$

We estimate the posterior distribution of α_C and β_C using the Metropolis-Hastings Markov Chain Monte Carlo (MCMC) method assuming uniform priors and having stored 1 in every 100 accepted values (thinning) and discarded the first 10,000 iterations (burn-in period). The mean and standard deviation of the time to viral clearance are given by $\mu_C = \alpha_C\,\beta_C$ and $\sigma_C = \alpha_C\,\beta_C^2$.

We assume that infectiousness in Zika infection starts 1.5 days before symptoms onset and finishes 1.5-2 days before virus becomes undetectable (reflecting the titer dependence of infectiousness) (*53*). We linearly scale the time dependence of the distribution obtained above by a factor $s = (\mu_{IP} - 1.5)/\mu_{IP}$, giving a human generation time with mean $\mu_h = s(\mu_{IP} + \mu_C)$ and standard deviation $\sigma_h = s\sqrt{\sigma_{IP}^2 + \sigma_C^2}$.

We report in Table S4 the resulting posterior estimates obtained for the mean and standard deviation of the human generation time and its components, having parameterized the distribution of the IIP as estimated in reference (*52*).

We use Gamma distributions to model the uncertainty in the IIP distribution parameters (median and dispersion of a lognormal distribution, as in (*52*)) with shape and scale parameters k_μ, θ_μ and k_σ, θ_σ respectively. These parameters were estimated by fitting (using least squares) the mean, 2.5th and 97.5th percentiles of the Gamma distributions to the estimated mean and credible interval bounds given in (*52*), giving estimates of k_μ = 53.10, θ_μ= 0.11 days, k_σ= 69.30 and θ_σ = 0.02 days (Table S4).

2.3 Extrinsic incubation period

Using Web of Science, we identified 6 papers (as of 22 April 2016) that report the susceptibility of *Aedes* spp mosquitoes to Zika virus (*54-59*). Of these papers, in three studies (*56-58*) mosquitoes were infected orally with Zika virus and sufficient information on the numbers of mosquitoes tested at each time interval post-infection was reported to allow the extrinsic incubation period (EIP) to be estimated. All three studies used the Uganda Zika strain, but different species of *Aedes* mosquitoes. Li *et al*.

(*56*) infected *Aedes aegypti* mosquitoes and sampled mosquitoes 1-7, 10 and 14 days post-infection. Wong *et al*. (*57*) infected *Aedes albopictus* mosquitoes and sampled the same time points as Li *et al*. Ledermann *et al*. (*58*) infected *Aedes hensili* and used a single sampling time 8 days post-infection; however, these authors used three replicate groups fed on blood with differing virus titers. In all cases, mosquito bodies and heads were tested for Zika virus separately, to determine whether infection had reached the midgut and salivary glands (SG) respectively. Given the data are so few, we combined data from all these experiments, thereby implicitly ignoring differences between species. We consider mosquitoes to be capable of transmitting Zika when the SG are infected, so the EIP is the time between infection and virus reaching the SG.

We assume that the EIP distribution can be represented using a Gamma distribution with shape parameter k_{EIP} and scale parameter θ_{EIP}, so that the cumulative probability of becoming infectious by day t is

$$F(t; k_{EIP}, \theta_{EIP}) = \frac{1}{\Gamma(k_{EIP})} \int_0^{t/\theta_{EIP}} s^{k_{EIP}-1} e^{-s} ds$$

where $\Gamma(k_{EIP})$ is the Gamma function evaluated at k_{EIP}.

We use the Bernoulli likelihood function to evaluate the probability that a mosquito is infectious by day t. The log-likelihood can be written as

$$\mathcal{L}(x|k_{EIP}, \theta_{EIP}) = \sum_{i=1}^{N} x_i \ln\big(F(t_i; k_{EIP}, \theta_{EIP})\big) + (1 - x_i) \ln\big(1 - F(t_i; k_{EIP}, \theta_{EIP})\big)$$

Here N is the total number of mosquitoes tested, t_i is the sampling time of the ith mosquito and x_i=1 if the mosquito tests positive for Zika virus in the SG and 0 otherwise.

The mean posterior estimates are k_{EIP} = 4.45 (95% credible interval (CrI): 2.53-7.12) and θ_{EIP} = 1.99 days (95% CrI: 1.09-3.5 days), which corresponds to a mean EIP of 8.2 days with a standard deviation of 4.0 days (Table S4). Fig. S4 shows the fitted probability density function, cumulative distribution function and data points.

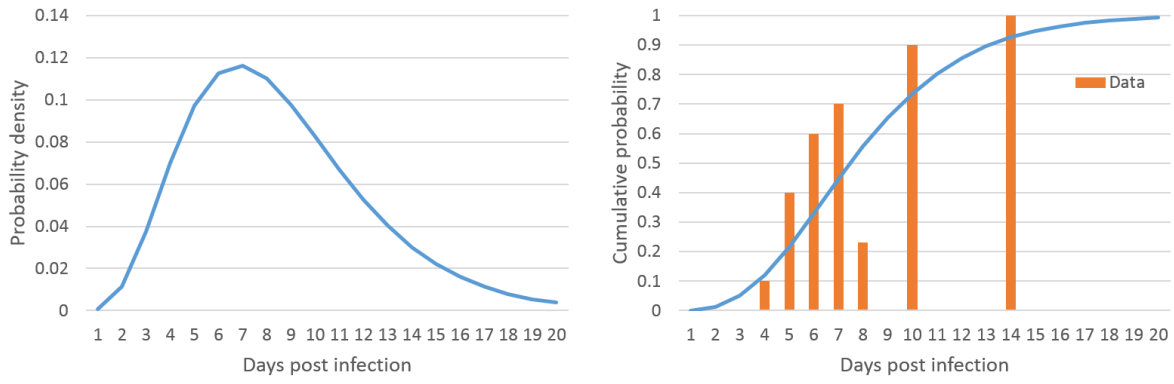

Fig. S4. Maximum likelihood EIP probability density function, and cumulative distribution function, with the aggregated proportion of mosquitoes reported infectious in the three studies shown as bars.

2.4 Mosquito-to-human generation time

We estimate the mean and standard deviation of the mosquito-to-human generation time distribution (*i.e.* the time between a mosquito being infected and it infecting a human), using the estimated EIP and the mosquito daily mortality rate ϵ. Given that the cumulative distribution function of the EIP is $F(t)$, the probability density function $f'(t)$ of a mosquito being infectious at time t is

$$f'(t) = \frac{F(t)}{\int_0^\infty F(t')dt'}$$

and the probability density function of the mosquito generation time *h(t)* is then

$$h(t) = \frac{f'(t)\exp(-\epsilon t)}{\int_0^\infty f'(t')\exp(-\epsilon t')dt'}$$

In order to estimate the mean μ_m and standard deviation σ_m of $h(t)$, we use the maximum likelihood estimates of the parameters defining $F(t)$ and the mean value of ϵ to construct $h(t)$ and then calculate μ_m and σ_m numerically. We assume that ϵ is Gamma distributed with a mean of 0.2/day and a standard deviation of 0.05/day so that the 5th and 95th percentiles are approximately 0.1/day and 0.3/day respectively, reflecting variability in published estimates of *Aedes aegypti* daily survival in Latin America (*60, 61*).

From this, we estimate that the mosquito-to-human generation time has mean μ_m = 11.3 days (95% CrI: 8.0 – 16.3 days) and standard deviation σ_m = 6.1 days (95% CrI: 3.9 -10.0 days) (Table S4). However, ϵ is likely to vary both seasonally and geographically which will affect both the generation time and R_0. When we calculate the overall generation time below, we estimate the uncertainty in the mean and standard deviation of the generation time distribution due to the variation in ϵ and the other model parameters.

2.5 Generation time for Zika virus

Combining the best estimates of the mean and standard deviation of the human-to-mosquito generation time with those of the mosquito-to-human generation time, we estimate that the overall distribution for the generation time of Zika virus (i.e. the time between infection of a human case and infection of the secondary human cases that case causes) has a mean of 20.0 days and a standard deviation of 7.4 days.

In order to compute the uncertainty in the mean and standard deviation estimates, we numerically sampled 100,000 realizations of the IIP (specifically, we sampled from the distribution of the parameters of the IIP (median and dispersion, as in (*52*)) and then used these realizations to estimate μ_{IP} and σ_{IP}) and of the mosquito generation time (specifically, from the joint posterior distribution of k_{EIP} and θ_{EIP} assuming uniform prior distributions on both parameters, and from the distribution of ϵ), which we then combined to reproduce the generation time distribution.

Table S4 summarizes the estimated mean and standard deviation of the overall generation time and its components and the uncertainty around these estimates. The standard deviation of the posterior distributions for the mean and standard deviation of the overall generation time were 2.3 and 1.3 days, respectively.

Table S4. Estimates of the mean and standard deviation of the generation time distribution and its components. All values have units of days. 95% credible intervals are given in parentheses.

	Mean	Standard Deviation
Intrinsic incubation period (IIP)	6.5 (4.8 – 8.5)	2.9 (1.0 – 5.5)
Time to viral clearance	4.7 (3.0 – 7.4)	4.0 (1.9 – 8.9)
Human-to-mosquito generation time	8.6 (6.2 – 11.6)	3.9 (2.0 – 7.4)
Extrinsic incubation period	8.2 (7.3 – 9.3)	4.0 (2.9 - 5.7)
Mosquito life time	5.0 (fixed)	1.7 (fixed)
Mosquito-to-human generation time	11.3 (8.0 – 16.3)	6.1 (3.9 – 10.0)
Zika virus generation time	20.0 (15.6 – 25.6)	7.4 (5.0 – 11.2)

3. Estimation of the reproduction number, *R*

We estimate the instantaneous reproduction number *R* in time for each Latin American country reporting confirmed and/or suspected Zika cases in at least 6 weeks from 4 January 2015 to 28 May 2016 using the total (confirmed plus suspected) weekly case incidence and the generation time distribution statistics estimated in section 2.5.

The instantaneous reproduction number *R* was computed over 5-week sliding windows using the method presented in reference (*62*). In brief, the instantaneous reproduction number *R* of each time window is computed as the median of the weekly instantaneous reproduction number weighted by the weekly incidence. We plot *R* centered on the middle week of the 5-week window used to compute each estimate.

The analysis was conducted in R (version 3.3.0) using the package 'EpiEstim', having selected the 'UncertainSI' option in the function EstimateR(), which was parameterized using the estimates presented in section 2.5 and using a prior distribution for *R* with mean and standard deviation set to 5.

For reference, we provide the R code used to generate the estimates of *R* presented in this paper as an additional Supplementary Material file.

4. Transmission model specification

It should be emphasized that our aim is not to construct a geographically detailed model of Zika transmission in Latin America (which would require an individually-based microsimulation); instead we aim to capture what is known about the fundamental epidemiology of Zika, drawing on lessons from dengue where necessary, and use a highly simplified representation of the geography of the continent to explore the sensitivity of model results to assumptions about population connectivity, transmission intensity and the impact of control measures and cross-immunity with dengue.

We model Zika transmission in an age-stratified host population structured into a set of N_p spatial patches each with human population size N. Table S5 lists the state variables of the system, while table S6 lists model parameter and assumed values (plus sources for those values). We denote incidence rates with the suffix '*c*'.

Table S5. State variables of transmission model, where *i* refers to patch and *t* and *a* refer to time and age, respectively.

Symbol	Description
$\boldsymbol{S_i(t,a)}$	Number of susceptible people of age a at time t in patch i
$\boldsymbol{R_i(t,a)}$	Number of immune people of age a at time t in patch i
$\boldsymbol{cI_i(t,a)}$	Incidence of infection in people of age a at time t in patch i
$\boldsymbol{L_i(t)}$	Number of larval stage female mosquitoes in patch i
$\boldsymbol{A_i(t)}$	Number of uninfected adult female mosquitoes in patch i
$\boldsymbol{H_i^j(t)}$	Number of adult female mosquitoes incubating infection in incubation stage j (=1,2) in patch i
$\boldsymbol{Y_i(t)}$	Number of infectious adult female mosquitoes in patch i

We assume that infection with Zika confers lifelong immunity to reinfection. In the deterministic formulation of the model, the time evolution of the human-related state variables is governed by the following set of partial differential equations:

$$\frac{\partial S_i}{\partial t} + \frac{\partial S_i}{\partial a} = -[\Lambda_i(t) + \mu(a)]S_i$$

$$\frac{\partial R_i}{\partial t} + \frac{\partial R_i}{\partial a} = \Lambda_i(t)\, S_i - \mu(a)R_i$$

Incidence is defined thus:

$$cI_i(t,a) = \Lambda_i(t)S_i$$

Parameterization of host demography is detailed below; in the equations above, $\mu(a)$ represents the mortality hazard experienced by an individual of age a. The force of infection on humans in patch I, Λ_i, is defined below.

Vector population dynamics followed a simple Ross-Macdonald type model:

$$\frac{dL_i}{dt} = bM_i - \alpha L_i - \omega L_i[1 + L_i/K_i(t)]$$

$$\frac{dA_i}{dt} = \alpha L_i - \Psi_i A_i - \epsilon_i(t) A_i$$

$$\frac{dH_i^1(t)}{dt} = \Psi_i A_i - (2\eta_i(t) + \epsilon_i(t))\, H_i^1$$

$$\frac{dH_i^2(t)}{dt} = 2\eta_i(t)\, H_i^1 - (2\eta_i(t) + \epsilon_i(t))\, H_i^2$$

$$\frac{dY_i}{dt} = 2\eta_i(t) H_i^2 - \epsilon_i(t)\, Y_i$$

Here M_i is the total adult female mosquito population size in patch *i*:

$$M_i = A_i + H_i^1 + H_i^2 + Y_i$$

The rate at which adult females produce female larvae is b, the mean development time of larvae is $1/\alpha$, and the larval mortality rate is ω.

We model seasonal climate variation as affecting three vector parameters:

- *Larval carrying capacity*, $K_i(t)$, where t is in years. We assume sinusoidal seasonal variation and that carrying capacity is proportional to the human population size in each patch, N:

  $K_i(t) = K_{0,i} N[1 + \Delta_i \cos(2\pi[t + \emptyset_i])]$

  Here $K_{0,i}$ is the average carrying capacity across the year (allowed to vary between patches to represent variation in Zika transmission intensity)

- *Vector mortality*, $\epsilon_i(t)$. We assume sinusoidal seasonal variation in lifespan, thus:

  $\epsilon_i(t) = \epsilon_0/[1 + \Delta_i \cos(2\pi[t + \emptyset_i])]$

  Here ϵ_0 is the mean daily death rate (see Table S6).

- *EIP*. We model an incubation rate, $\eta_i(t)$, using two incubation stages (each with duration $1/2\eta_i(t)$) to better approximate both the mean and standard deviation of the EIP distribution derived in section 2.3 above. We assume sinusoidal seasonal variation in the EIP:

  $\eta_i(t) = \eta_0/[1 - \Delta_i \cos(2\pi[t + \emptyset_i])]$

  Here η_0 is the mean incubation rate, set to the reciprocal of the mean EIP estimated in section 2.3 (see Table S6).

In the above equations, Δ_i and $\emptyset_i$ are the amplitude and phase of seasonal forcing for patch *i*, respectively. We assume that all three forms of seasonality are synergistic for Zika transmission (*i.e.* carrying capacity peaks at the same time that the EIP and vector mortality are at their minimum seasonal values) and that the phase and amplitude of all three are the same for any one patch *i*. These assumptions are a somewhat crude

simplification, but suffice to explore the overall impact of seasonal variation in transmission intensity on invasion dynamics.

We assign patch phase and amplitude parameters to mimic the seasonality of dengue transmission in Latin America. We assume a 4×5 grid of $N_p = 20$ patches. The top 8 (two rows of 4) patches are assumed to be above the equator with strong seasonality ($\Delta_i = 0.15$ and $\emptyset_i = 0$, giving a peak at the start of each year), 4 are assumed to be at the equator with weak seasonality ($\Delta_i = 0.05$ and $\emptyset_i = 0.25$, giving a small peak 3 months into the year) and 8 patches are assumed to be below the equator with strong seasonality ($\Delta_i = 0.15$ and $\emptyset_i = 0.5$, giving a peak in the middle of each year). Thus transmissibility is at a maximum in the Northern hemisphere patches at the time it is at a minimum in Southern hemisphere patches. System dynamics are not highly sensitive to the assumed phase parameters, but the amplitude of seasonal forcing strongly influences the duration of the initial epidemic.

We assign b by fixing the required value of R_m, the mosquito reproduction number, which can be shown to be given by:

$$R_m = \frac{\alpha}{\epsilon(\alpha + \omega)} b$$

The force of infection on mosquitoes in patch i, Ψ_i, is defined by:

$$\Psi_i = \frac{\kappa \beta_{hm}}{N} \int_0^{\infty} \int_{T_{\mathrm{IP}}}^{T_{\mathrm{IP}}+T_{\mathrm{Inf}}} \sum_{j=1}^{N_p} D_{ij} c I_j(t-\tau, a) \; d\tau da$$

Here T_{IP} is the intrinsic incubation period, T_{Inf} is the infectious period in humans, θ represents the factor by which infectiousness of symptomatic infection exceeds that of asymptomatic infections, κ is the biting rate per adult female mosquito, β_{hm} is the per bite transmission probability from humans to mosquitoes and N is the human population size of each patch.

D_{ij} represents epidemiological coupling between spatial patches; we assume: (i) that most transmission is within patch, (ii) that a small fraction of contacts, d_{nn}, occur with nearest-neighbor patches and (iii) that an even smaller proportion of contact, d_{global}, are between all patches (including nearest neighbors). Hence:

$$D_{ij} = \left(1 - d_{nn} - d_{global}\right)\delta_{ij} + d_{nn} C_{ij} + d_{global}$$

Here $\delta_{ij} = 1$ if $i = j$ and 0 otherwise, $C_{ij} = 1/nn_i$ if j is adjacent to i (with nn_i being the number of nearest neighbors of i), and 0 otherwise.

The force of infection on humans, Λ_i, is defined by:

$$\Lambda_i = \lambda_{import} + \frac{\kappa \beta_{mh}}{M_i} Y_i$$

Here λ_{import} is the force of infection resulting from imported human cases of Zika from outside the continent. We choose to represent this as a force of infection on humans to more easily control the total rate at which infection is seeded in humans in the modelled population. β_{mh} is the per bite transmission probability from mosquitoes to humans and M_i is the total adult female mosquito size.

The basic reproduction number in patch i, R_{0i}, is then given by

$$R_{0i} = \frac{\kappa^2 \beta_{mh} \beta_{hm} T_{\text{Inf}}}{\epsilon_0 (1 + \epsilon_0/\eta)} m_i$$

Here $m_i = M_i/N$, the number of adult female mosquitoes per person in patch i. In the absence of seasonal forcing of carrying capacity, the equilibrium value of m_i is given by:

$$m_{eq,i} = \frac{\alpha}{\epsilon_0} \left[\frac{\alpha(b - \epsilon)}{\epsilon_0 \omega} - 1 \right] K_{0,i}$$

$K_{0,i}$ is assigned by fixing the required value of $m_{eq,i}$ and inverting this equation.

We vary R_0(the reproduction number of Zika) by adjusting the value of β_{hm} to set an overall mean value across patches, then vary R_0 between patches by varying $m_{eq,i}$. R_0 could equally well have been varied by adjusting β_{hm}, κ or m_{eq} (or a combination of all four); all give exactly identical results for the modelling shown here.

Table S6 lists all model parameters, assigned values and sources for these. We note that for a given transmission intensity (R_0), model results presented in this paper are very weakly sensitive to the values of entomological parameters.

Table S6. Parameters of transmission model. Estimated parameters are indicated or assigned values are listed.

Symbol	Description	Estimated or value if assigned	Source references
$\boldsymbol{\mu(a)}$	Human hazard of death at age a	Fitted to Brazilian demography	See text below
$\boldsymbol{B}$	Human birth rate	Assigned to give fixed equilibrium population size of 30 million in each patch	See text below
$\boldsymbol{R_m}$	Mosquito (*Aedes aegypti*) reproduction number	2.69 based on estimate of female fecundity of 0.269/day and adult mortality rate of 0.1/day	(*63*)
$\boldsymbol{b}$	Rate at which adult female mosquitoes produce female larvae	Assigned to match required value of R_m	N/A
$\boldsymbol{1/\alpha}$	Mean development time of mosquito larvae	19 days	(*63*)
$\boldsymbol{1/\eta_0}$	Mean EIP	8.4 days – slightly modified from the value of 8.1 given in section 2.3 to allow the two-stage representation of incubation used in the transmission model to better approximate the mean and	See Section 2.3.

		standard deviation of the overall mosquito generation time derived in that section	
$\boldsymbol{\omega}$	Larval mosquito mortality rate	0.025/day	(*64*)
$\boldsymbol{\epsilon_0}$	Mean adult mosquito mortality rate	0.2/day	(*65*)
$\boldsymbol{m_{eq,i}}$	Equilibrium number of adult female mosquitoes per person in patch *i* in the absence of seasonal variation in carrying capacity	Randomly selected at the start of each model run from a lognormal distribution with mean 1.5 (typical of endemic settings) and coefficient of variation of 0.15 (to crudely represent geographic variation in transmission intensity between patches)	(*66*)
$\boldsymbol{K_{0,i}}$	Mean larval mosquito carrying capacity	Assigned to match required value of $m_{eq,i}$	N/A
$\boldsymbol{\Delta_i}$	Relative amplitude of seasonal variation in carrying capacity, vector mortality and EIP	Assigned value of 0.15 for 8 'Northern hemisphere' patches, 0.05 for 4 'equatorial' patches, and 0.15 for 8 'Southern hemisphere' patches	Assumed, based on dengue incidence seasonality
$\boldsymbol{\emptyset_i}$	Phase (in years) of seasonal variation in carrying capacity, vector mortality and EIP	Assigned value of 0 for 8 'Northern hemisphere' patches, 0.35 for 4 'equatorial' patches, and 0.5 for 8 'Southern hemisphere' patches	N/A
$\boldsymbol{T}_{\mathrm{IP}}$	Intrinsic incubation period	5.5 days – assigned with T_{Inf} to approximately match mean and standard deviation of human generation time distribution detailed in section 2.5	See section 2.5
$\boldsymbol{T}_{\mathrm{Inf}}$	Infectious period in humans	6 days – assigned with T_{IP} to approximately match mean and standard deviation of human generation time distribution detailed in section 2.5	See section 2.5
$\boldsymbol{\beta_{hm}}$	Per bite transmission probability from humans to mosquitoes	Assigned as 0.7 to give a mean seasonal peak R_{0i} (given values of Δ_i) of 4.1 and an annual mean R_{0i} of 2.3.	N/A

$\boldsymbol{\beta_{mh}}$	Per bite transmission probability from mosquitoes to humans	Arbitrarily set to 0.7 (for fixed R_{0i}, varying this parameter does not affect model dynamics)	N/A
$\boldsymbol{R_{0i}}$	Zika reproduction number in patch *i*	Average seasonal mean value across patches of 2.3 (mean peak seasonal value of 4.1) for default results (with coefficient of variation across patches of 0.15), varied in sensitivity analysis. This results in peak seasonal R_{0i} values in the approximate range 2.2 to 6.2, and seasonal minimum values in the range 0.7 to 2.1.	See section 3
$\boldsymbol{\kappa}$	Biting rate per mosquito	0.5/day (for fixed R_{0i}, varying this parameter has a limited effect on model dynamics)	(*67, 68*)
$\boldsymbol{N_p}$	Number of spatial patches	20 on 4 × 5 grid	Assumed
$\boldsymbol{N}$	Human population of each patch	30 million, to give 600 million total human population (approximately that of Latin America)	Assumed
$\boldsymbol{d_{nn}}$	Proportion of transmission which is with nearest neighbor patches	0.005, varied in sensitivity analysis	Assumed
$\boldsymbol{d_{global}}$	Proportion of transmission which is between all patches	0.0005, varied in sensitivity analysis	Assumed
$\boldsymbol{\lambda_{import}}$	Force of infection on humans resulting from imported cases of Zika in travelers visiting Latin America from elsewhere	10^{-8}/year – giving 6 imported case per year overall	Assumed

Demographic parameters were calibrated to approximate the population age distribution of the most populous Latin American countries, under the simplifying assumption that population size is constant over time. Fig. S5 shows the match of the modelled population age distribution to the age distribution of the populations of Brazil, Mexico, Colombia and Argentina.

We simulated the stochastic version of the model detailed above, using a discrete time approximation and a time step of 1 day. To reduce the computational requirements of the simulation, we approximated the continuous representation of age given in the model specification detailed above with discrete 10-year age classes.

Initial conditions were set to the equilibrium age distribution and assuming an initially entirely susceptible population.

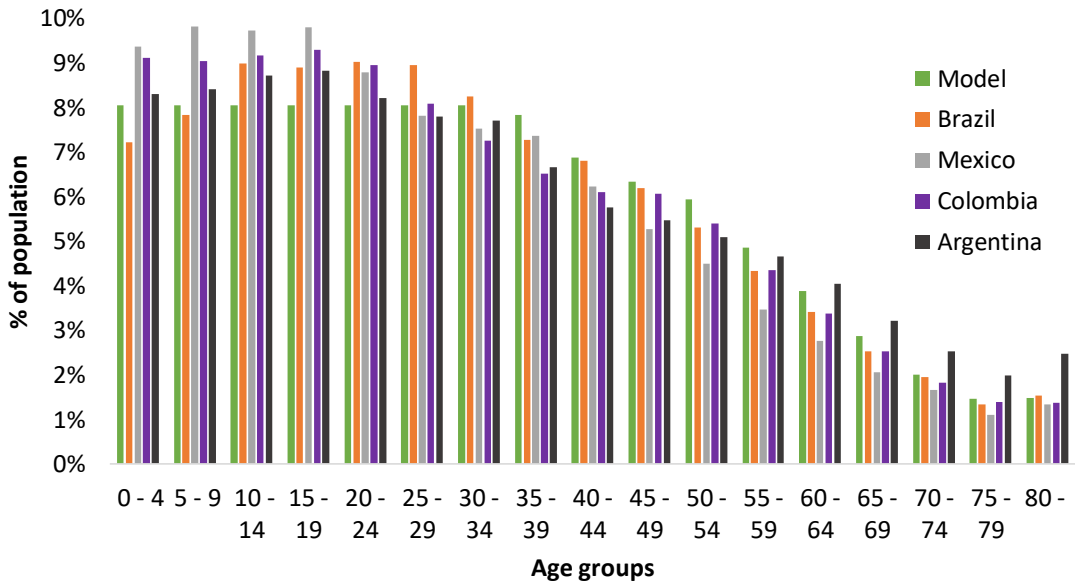

Fig. S5. Comparison of modelled age distribution and age distributions of Brazil, Mexico, Colmbia and Argentina in 2015 (UN World Population Prospects 2015 - http://esa.un.org/unpd/wpp/).

Supplementary Results

5. Estimation of the reproduction number, *R*

Fig. S6 mirrors Fig. 1 of the main text and shows reported weekly clinically suspected Zika case incidence and *R* estimates for the ten states in Brazil for which case data were publically available. Laboratory confirmed case incidence was not available for Brazil. Figure S7 shows suspected and laboratory confirmed Zika case incidence and *R* estimates for all Latin American and Caribbean countries for which surveillance data were publically available. Despite surveillance limitations (i.e. low levels of laboratory confirmation and changes in surveillance sensitivity over time), a relatively consistent picture is seen: estimates vary between approximately 1.5 and 6, similar to published values for Zika in French Polynesia.

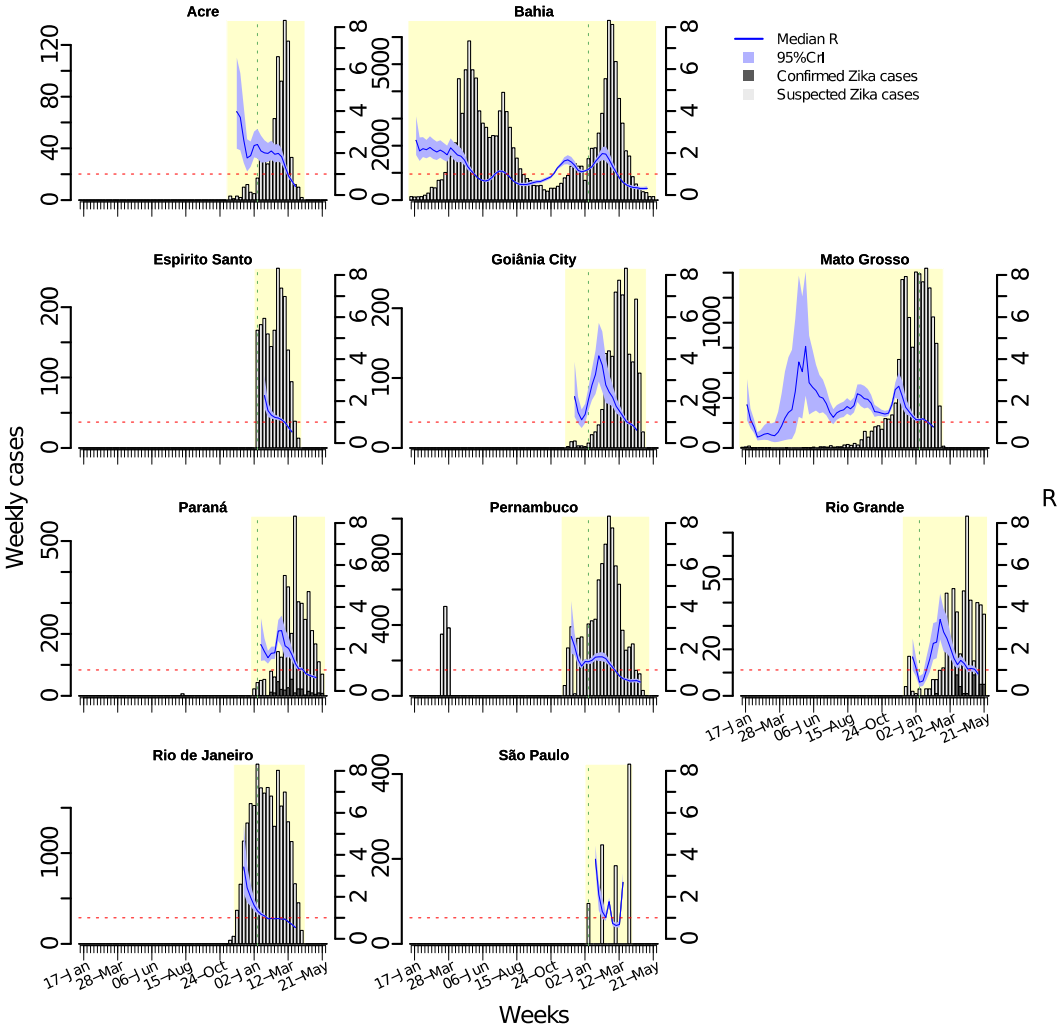

Fig. S6. Publically available surveillance data on weekly clinically suspected Zika cases (laboratory confirmation not generally available) for 10 Brazilian states (left axis and bars) overlaid with estimates of the reproduction number, *R*, over time (right axis, running 5-week average shown, centered on the middle week). Blue shaded areas show 95% credible intervals around the median estimated *R*. Yellow shading shows the period over which the incidence data were used to estimate *R*. The vertical dashed line marks the first week of 2016 and the horizontal dashed line marks the threshold value of *R* =1.

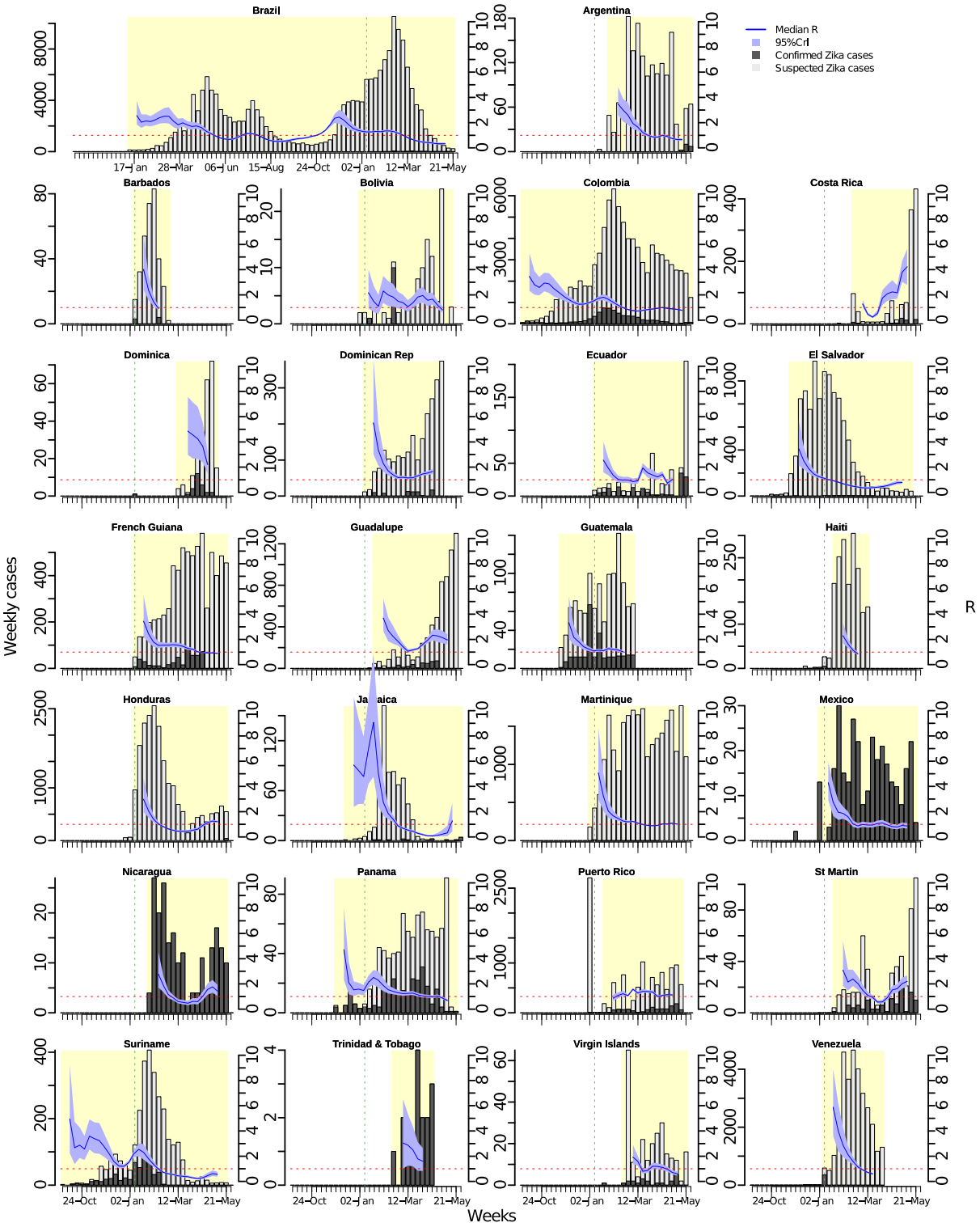

Fig. S7. Publically available surveillance data on weekly suspected (clinically diagnosed but without laboratory confirmation) Zika cases (light grey) and laboratory confirmed (dark grey) Zika cases (left axis and bars) overlaid with estimates of the reproduction number, *R*, over time (right axis, running 5-week average shown, centered on the middle week). Results for 26 Latin American and Caribbean countries are shown.. Blue shaded areas show 95% credible intervals around the median estimated *R*. Yellow shading shows the period over which the incidence data were used to estimate *R*. The vertical dashed line marks the first week of 2016 and the horizontal dashed line marks the threshold value *R* =1.

6. Additional model results

6.1 Impact of stochasticity on modelled dynamics

Fig. S8 illustrates that model dynamics show substantial stochastic variation, particularly in the scale of the initial epidemic and thus (because of the resulting variation in the level of herd immunity which has accumulated) in the timing of the reoccurrence of large-scale transmission.

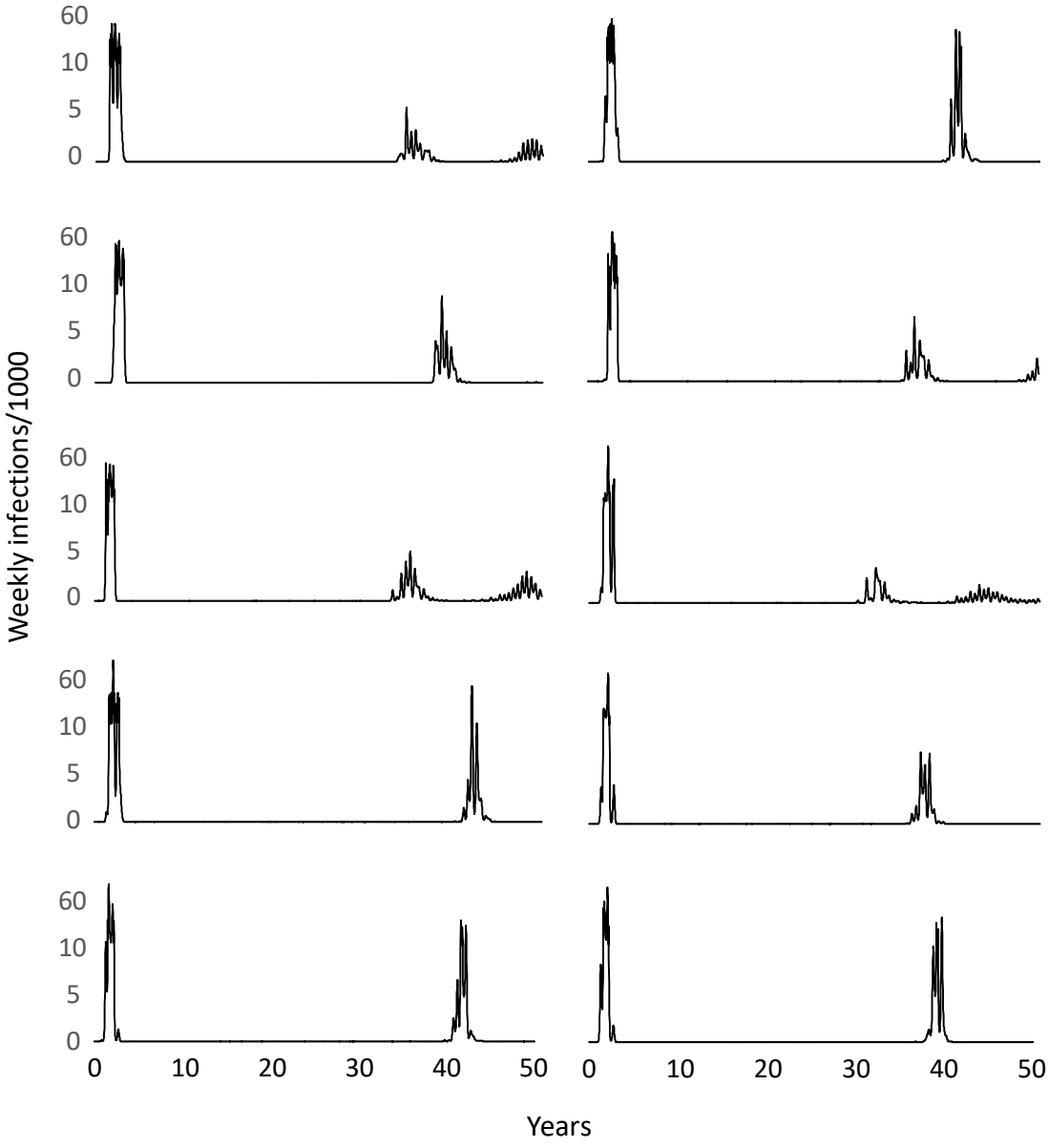

Fig. S8: Ten realizations of the stochastic model in the absence of interventions (as the upper blue curve of Fig. 2 in the main text, which corresponds to the bottom right realization here). Smaller initial epidemics are associated with a faster resumption of transmission, though the delay never falls below approximately 20 years. Incidence is plotted on a non-linear scale (increments of 2 up to 10, then increments of 20) to allow later epidemics to be resolved clearly.

This variation is driven by the seasonal variation in the transmission intensity of Zika assumed by the model. Seeding of infection is random, leading to variability in the starting time of the initial epidemic. If the start time is such that the peak of the epidemic coincides with the seasonal trough in transmissibility, then the scale of the initial epidemic is reduced, leading to a smaller delay until epidemic transmission restarts, since fewer new susceptible individuals need to be born into the population.

If seasonal variation is less than we assume (see model definition section above), then the variability shown in Fig. S8 is reduced.

The high level of variability seen between different model realizations limits the value of averaging over large numbers of simulations since the average incidence time-series thus calculated is very different from any single run. In the sensitivity analyses below we therefore present ten simulations in each case and highlight the qualitative impacts on modelled dynamics of changing key model parameters.

6.2 Sensitivity of dynamics to transmission intensity

Our baseline simulations assume that transmission intensity (R_0) varies spatially (i.e. between patches) and seasonally. The seasonal average R_0 is assigned randomly from a lognormal distribution with mean 2.35 and coefficient of variation (standard deviation/mean) of 0.15. This gives a spread across patches of seasonal average R_0 values in the approximate range 1.7 to 3.2. Seasonality in larval carrying capacity and vector competence (see section 4) then causes R_0 to vary between a 1.6 and 3.2 when the seasonal mean is 2.35 (the default). Combining seasonality with spatial variation results in peak seasonal R_0 values in the approximate range 2.4 to 4.2, and seasonal minimum values in the range 1.2 to 2.2. These values are broadly compatible with the estimates presented in Fig. 1 of the main text and result in our simulation giving a modal timescale for the initial epidemic of 2 years.

However, since our peak estimates of R_0 are sometimes as high as 6 (Figs. 1, S6, S7), we also explored a scenario where transmissibility was increased by 50% over the baseline values (implemented by scaling $m_{eq,i}$, defined in Table S6, by a factor of 1.5). Fig. S9 illustrates the effect this change has on model dynamics – the initial epidemic occurs substantially faster (often within a single year) and the peak weekly infection incidence is approximately doubled.

Moreover, increasing R_0 reduces the delay from the initial epidemic to when large-scale transmission restarts. This is a fundamental consequence of the underlying transmission dynamics (Fig. S10); as R_0 increases above approximately 2, the gap lessens between the total proportion of the population infected in an epidemic (termed the final size or cumulative attack rate) and the threshold proportion of the population who need to have been infected for herd immunity to stop transmission (the critical vaccination proportion, $1 - 1/R_0$). This means it takes fewer years of new births to increase the susceptible pool (and thus R) to the level which allows transmission to restart.

More generally, Fig. S10 gives an important insight into the ability of flaviviruses to persist in human populations; values of R_0 which are typical of flaviviruses (i.e. 1.5-5) cause explosive epidemics but then generate long periods when herd immunity

prevents further transmission. An important topic for future work is exploring whether this is a potential explanation of why only dengue (the persistence of which is potentially increased by immune-mediated interactions between serotypes) maintains endemicity in human populations without the need for reseeding from a zoonotic reservoir.

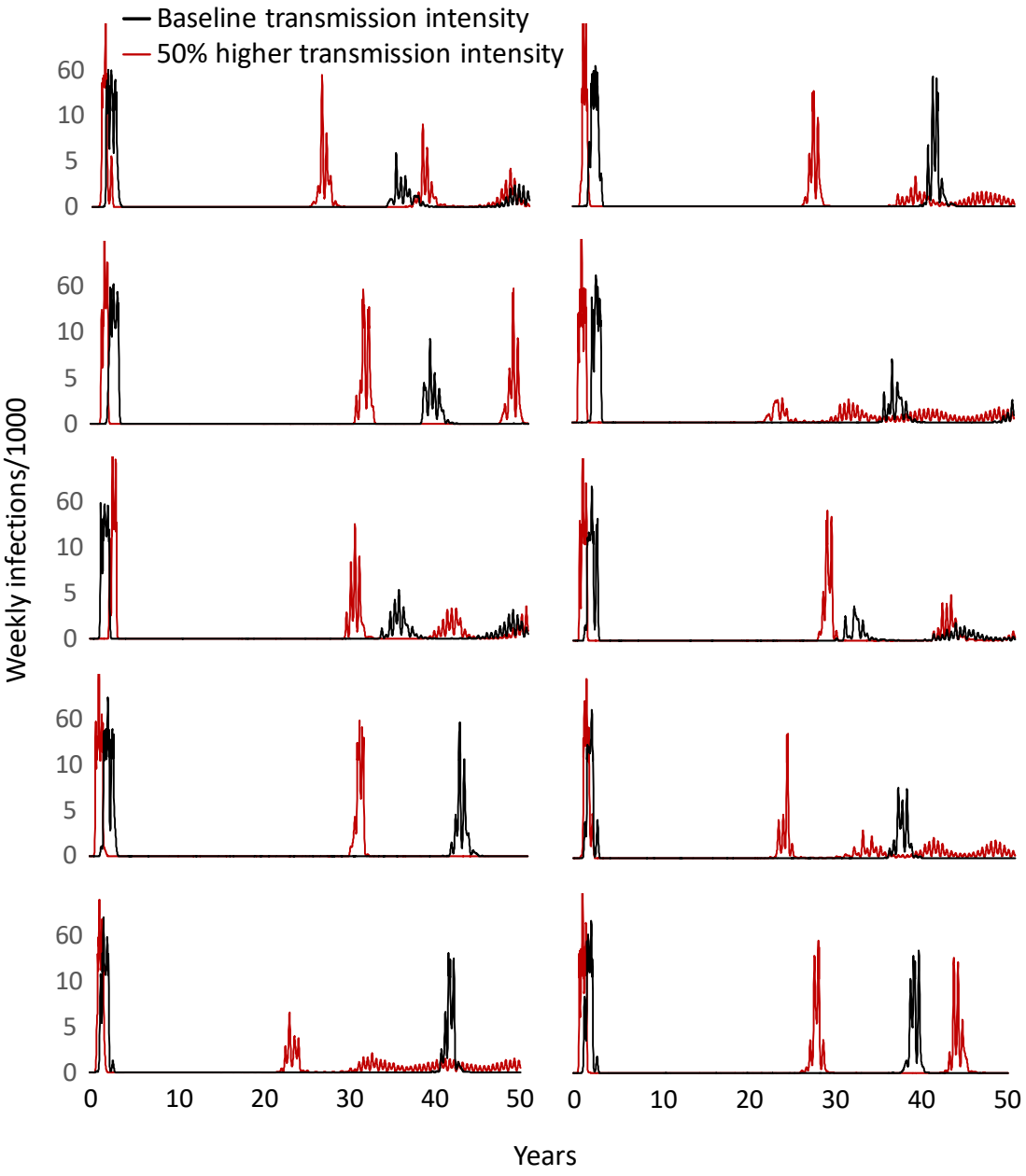

Fig. S9: As Fig. S8, but overlaying matching runs (generated with the same random number seeds) for which R_0 was increased by 50%. The peak incidence (and cumulative attack rate) of the initial epidemic increases while its duration decreases. The delay from the end of the initial epidemic to the restarting of transmission is also reduced.

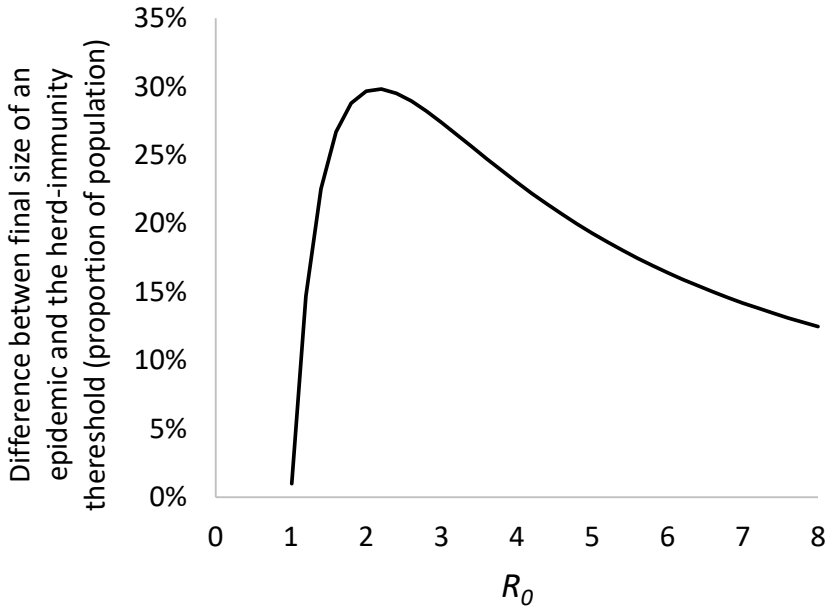

Fig. S10: Difference between the final size of an epidemic (in the absence of seasonality or spatial variation in transmissibility) and the proportion of the population that needs to be immune to cause *R* to fall to 1 and transmission to stop, plotted as a function of R_0. This quantity monotonically determines the delay from the end of the initial epidemic to when large-scale transmission restarts, as it quantifies the proportion of the population which needs to be replenished with new births to cause the susceptible pool to increase to the level required for *R* to exceed 1.

6.3 Impact of controls imposed during the initial epidemic

Control measures which reduce transmission, but not sufficiently to achieve $R_0 < 1$, will reduce the total proportion of the population infected in the initial epidemic. This has the benefit of reducing disease burden, but the downside of decreasing the level of herd immunity which is accumulated in the epidemic – meaning it takes fewer years for new births to replenish the susceptible pool and allow transmission to restart.

While such interventions have a consistent qualitative impact on the transmission dynamics (Fig. S11), the precise magnitude depends on the timing and effectiveness of control measures, and the timing of the epidemic overall. If the initial epidemic is already smaller than the average due to the impact of seasonality in transmission intensity, then the impact of control measures is reduced (Fig. S11).

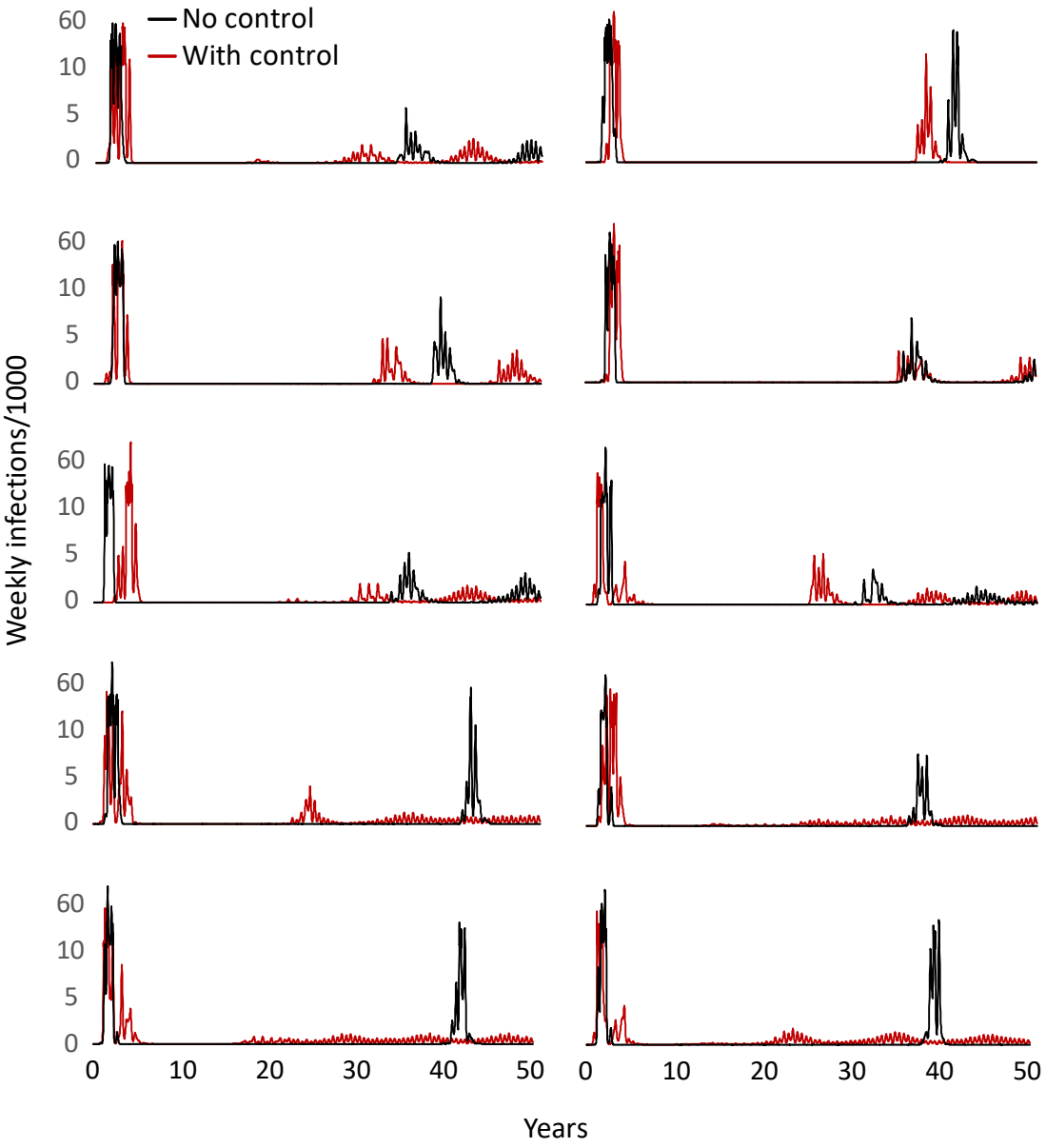

Fig. S11: As Fig. S8, but overlaying matching runs (generated with the same random number seeds) which model one year of vector control during the initial epidemic, the effect of which is to decrease mean mosquito lifespan by 20%. In most model realizations, this transient intervention reduces the scale but increases the duration of the initial epidemic and decreases the delay from the end of the initial epidemic to the restarting of transmission.

It should be noted that while more effective interventions can extend the duration of the initial epidemic still further (particularly if they do reduce R to <1 when in place), they do not necessarily further shorten the delay to the next epidemic.

6.4 Impact of cross-immunity from exposure to other flaviviruses

Both cross-protection and antibody-dependent enhancement due to population exposure to other flaviviruses (notably dengue) might modify the transmission dynamics of Zika. The evidence for such interactions is currently limited and mixed; a case control study showed no effect of prior exposure to dengue on the risk of Guillain-Barré syndrome following Zika infection in French Polynesia (*69*), while *in vitro* studies show some evidence that dengue antibodies can enhance Zika virus replication (*11*)

Here we explore the simplest scenario: that when the Zika epidemic began in Latin America, individuals who had previously experienced infection with one specific dengue serotype had reduced susceptibility to Zika. We model this by crudely assuming the proportion of people of age a with prior exposure is $1 - \exp(-\lambda_d a)$, where λ_d is the average force of infection for that serotype, here assumed to be 0.025/year. We then assume that 25% of individuals with prior exposure are immune to Zika at the start of the epidemic. We do not attempt to model the long-term dynamics of co-circulation of dengue and Zika; thus our model is principally examining the impact of cross-protection on the initial epidemic.

The impact of such cross-immunity is shown in Fig. S12, and is similar to the impact of the intervention scenario considered in section 2.3 above (Fig. S11): a decrease in scale of the initial epidemic and a shorter delay from the end of the initial epidemic to the resumption of large-scale transmission.

However, this effect is not always observed – in some model realizations, cross-immunity perturbs the timing of the initial epidemic such that the epidemic peak occurs when R_0 is at its seasonal maximum, resulting in a larger overall epidemic than otherwise, and thus causing a longer delay after the initial epidemic until the resumption of transmission.

More generally, antibody-dependent enhancement and cross-protection might cause dengue and Zika transmission dynamics to interact in complex and counter-intuitive ways; however, more realistic (and complex) modelling of the co-circulation of Zika and dengue will be needed to rigorously explore the dynamical consequences of such interactions.

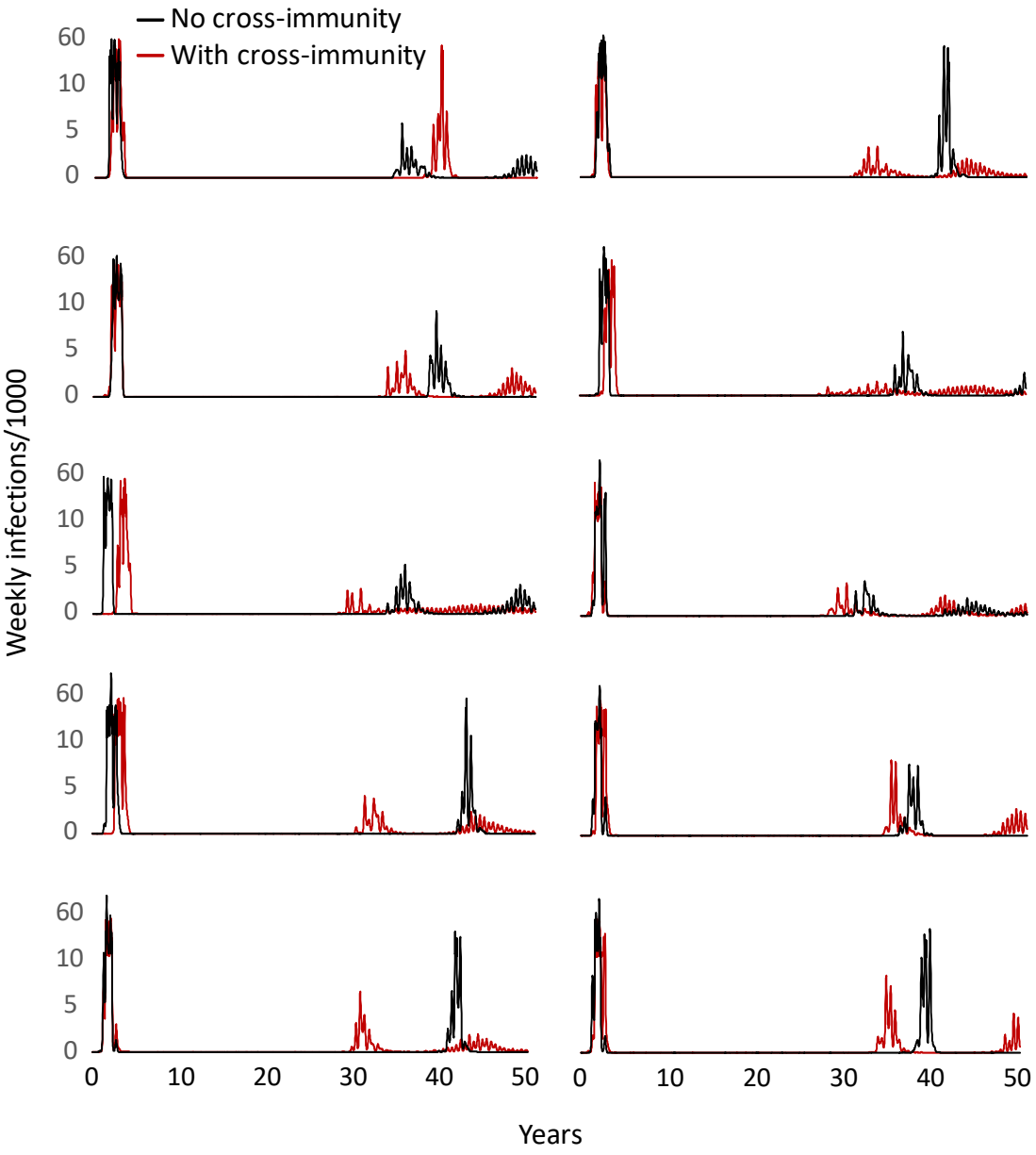

Fig. S12: As Fig. S8, but overlaying matching runs (generated with the same random number seeds) which include some cross-immunity in the host population due to prior exposure to other flaviviruses.

6.5 Impact of population connectivity

Here we have used a simple 'patch' model to represent geographic heterogeneity and locality of contact patterns. We model Latin America as 20 patches, each with a population of 30 million people, on 4 × 5 grid. Most transmission occurs within a patch, but a small proportion of infectious contacts occur between patches: our default assumption is that 0.5% of infectious contacts occur between nearest-neighbor patches, and 0.05% occur randomly across the entire modelled population.

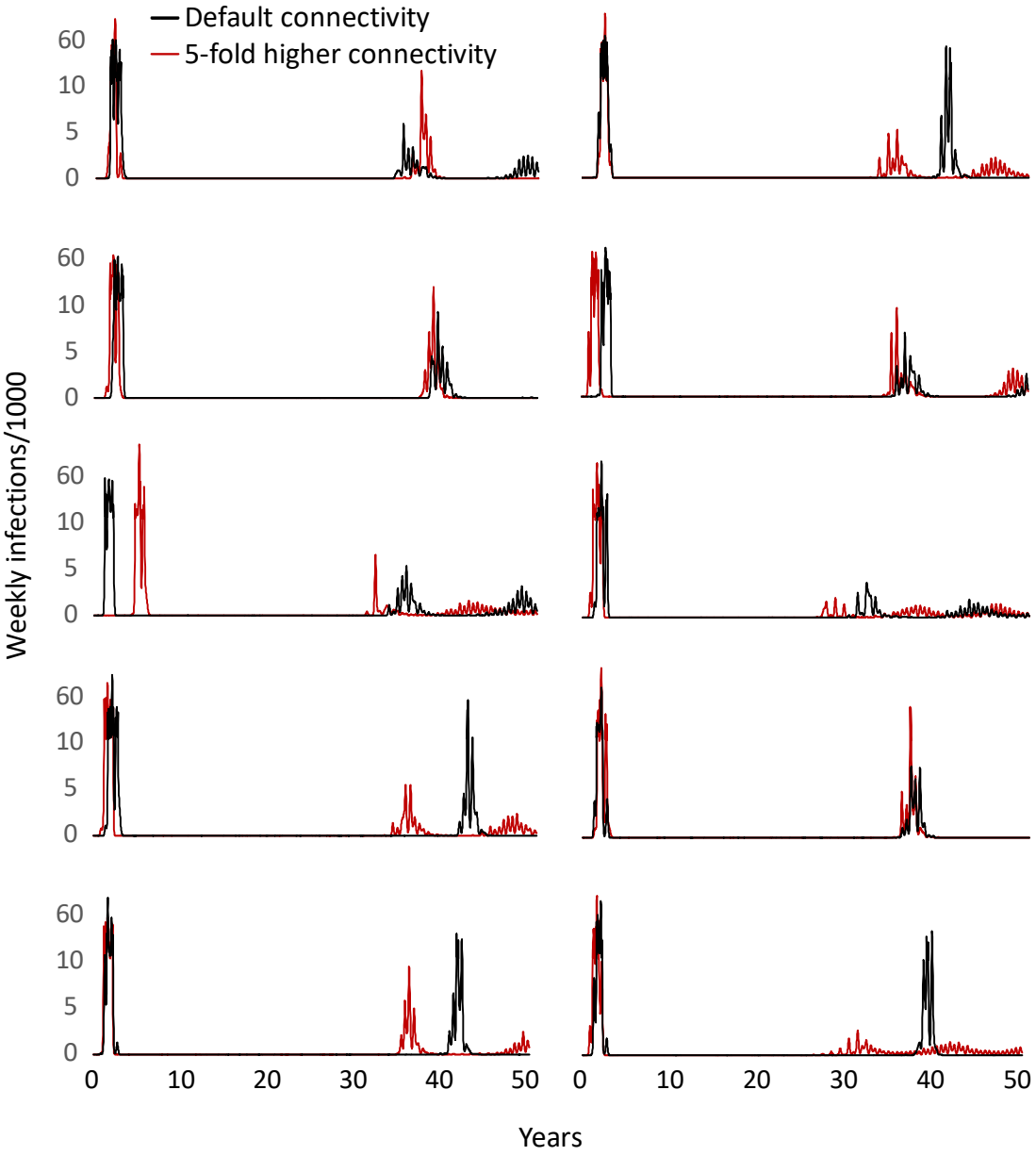

Fig. S13: As Fig. S8, but overlaying matching runs (generated with the same random number seeds) for which between patch contacts have been increased five-fold relative to their default values.

To put these values into context, Brazil (with a population of 200 million) receives approximately 6 million tourist visits per year (source: World Bank - http://data.worldbank.org/indicator/ST.INT.ARVL). Assuming each visit last 2 weeks, a proportion $(6 \times 2)/(200 \times 52)$=0.135% of people in Brazil at any one time are tourists. Assuming similar numbers of outbound tourists (Brazilians travelling overseas) who might bring home infection, this number rises to 0.27%. Doubling again to account for shorter but more frequent cross-border journeys and business travel gives values similar to those we have assumed.

However, this calculation does not allow for within-country travel; with a population of 200 million, Brazil accounts for 7 of the 20 patches being modelled. We therefore explore the sensitivity of modelled dynamics to a five-fold increase in out-of-patch contacts; *i.e.* that 2.5% of infectious contacts occur between nearest-neighbor patches, and 0.25% occur randomly across the entire modelled population. Fig. S13 shows that the invasion dynamics of Zika are relatively insensitive to even this large change in connectivity. This gives some reassurance on the robustness of our results despite our use of a highly simplified representation of geographic space and population movements.

6.6 Impact of direct human-to-human transmission

Possible sexual transmission of Zika has been documented (*51*). We therefore explored the effect of a small level of direct human-to-human transmission on epidemic dynamics. We assumed that the human population experienced a small proportion of the human-to-mosquito force of infection, Ψ_i, such that the basic reproduction number for direct human-to-human transmission was 0.2. This is equivalent to assuming a 20% chance that an infected individual will infect their sexual partner, making the simplifying assumption that the mean number of sexual partners per person is 1 over the timescale of a single Zika infection. When including human-to-human transmission, we adjusted human-to-mosquito transmission rates to keep overall mean reproduction numbers unchanged.

Fig. S14 shows that including such transmission has a relatively minor effect on system dynamics: there may be a hint of a reduction in the delay to when transmission restarts after the primary epidemic, perhaps because human-to-human transmission slightly reduces the effect of seasonal variation in vector dynamics on transmission.

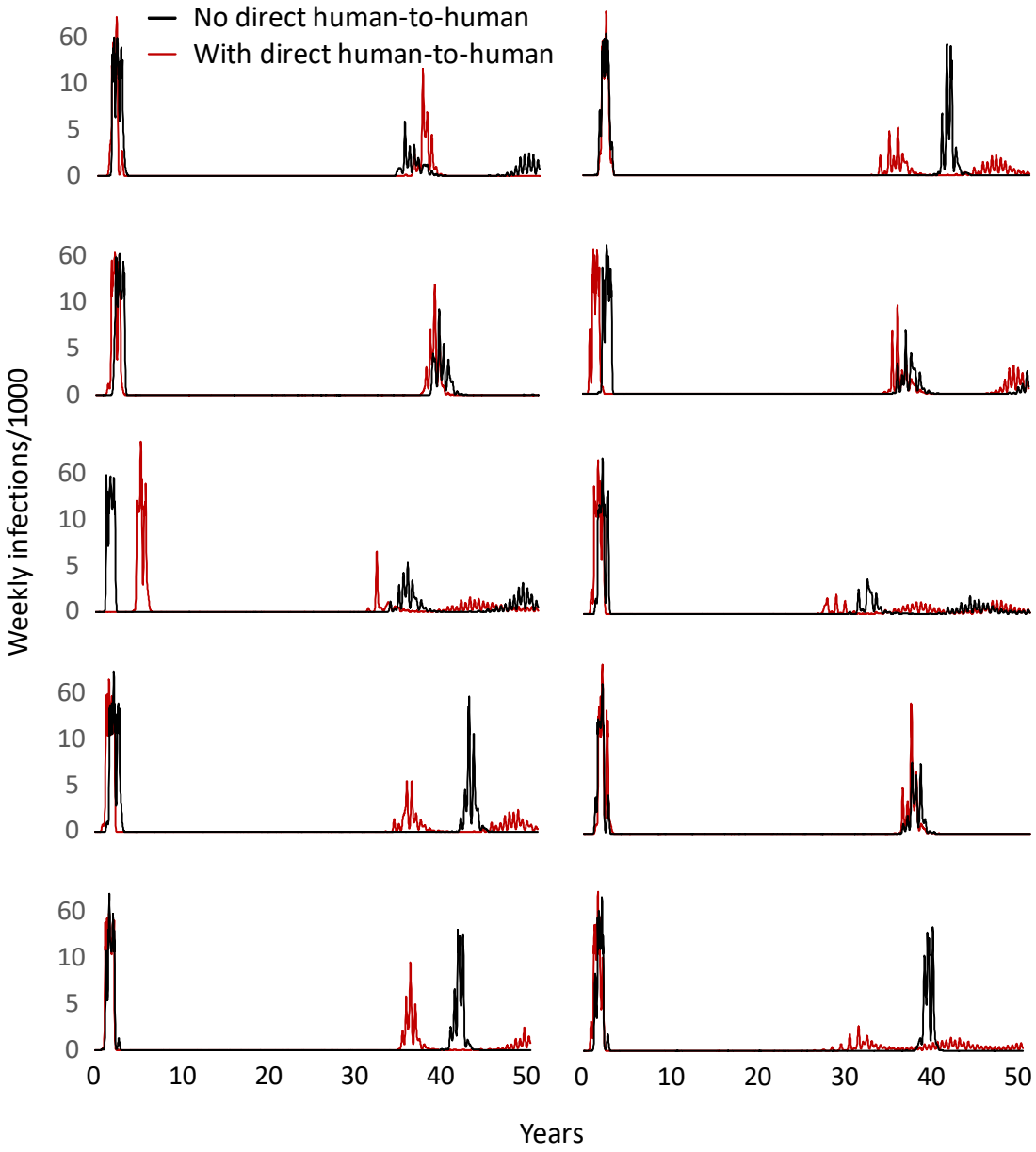

Fig. S14: As Fig. S8, but overlaying matching runs (generated with the same random number seeds) for which a low level of direct human-to-human transmission had been incorporated into the model (see text).

7. References

12. Panamerican Health Organization, “Cumulative Zika suspected and confirmed cases reported by countries and territories in the Americas, 2015-2016. Updated as of 02 June 2016” (2016). http://ais.paho.org/phip/viz/ed_zika_cases.asp
13. Panamerican Health Organization, “Zika in the Americas. New cases by Epidemiological Week. Updated as of 02 June 2016” (2016). http://ais.paho.org/phip/viz/ed_zika_epicurve.asp
14. Instituto Nacional de Salud Colombia, “Conteo de casos por munciipio y semana” (2016). http://www.ins.gov.co/Noticias/Paginas/Zika.aspx#.Vx9_mPkrKUk
15. Dirección General de Epidemiología Secretaría de Salud de México, “Casos Confirmados de Infección por Virus Zika, Semana Epidemiológica No.15 de 2016.” (2016). http://www.epidemiologia.salud.gob.mx/dgae/avisos/zika.html
16. Ministerio de Salud Publica República Dominicana, “Boletines epidemiológicos semanales. Dirección General de Epidemiología” (2016). http://digepisalud.gob.do/docs/Boletines epidemiol%c3%b3gicos/Boletines semanales/
17. Minsal Dirección de Vigilancia Sanitaria, “Boletines epidemiológicos 2016, El Salvador” (2016). http://www.salud.gob.sv/direccion-de-vigilancia-sanitaria-2/
18. Ministerio de Salud de la República de Panamá, “Boletín Epidemiológico No 13 Zika” (2016). http://www.minsa.gob.pa/sites/default/files/publicacion-general/boletin_13_zk.pdf
19. Secretaría de Salud Honduras, “Informe de Situación del Dengue, Chikungunya y Zika a la semana No.13” (2016). http://www.redhum.org/documento_detail/secretaria-de-salud-informe-de-situacion-del-dengue-chikungunya-y-zika-a-la-semana-no13
20. Secretaria de Vigilância em Saúde − Ministério da Saúde, “Monitoramento dos casos de dengue, febre de chikungunya e febre pelo vírus Zika até a Semana Epidemiológica 13, 2016” *2358-9450* (2016). http://combateaedes.saude.gov.br/images/sala-de-situacao/2016-013-Dengue-SE13.pdf
21. Secretaria de Vigilância em Saúde − Ministério da Saúde, “Monitoramento dos casos de dengue, febre de chikungunya e febre pelo vírus Zika até a Semana Epidemiológica 16, 2016” *2358-9450* (2016). http://combateaedes.saude.gov.br/images/boletins-epidemiologicos/2016-013-Dengue-SE16.pdf
22. The World Bank, “Population total” (2016). http://data.worldbank.org/indicator/SP.POP.TOTL
23. Instituto Brasileiro de Geografia e Estatística, “Resident population in Brazil 2015” (2015). http://www.ibge.gov.br/english/estatistica/populacao/estimativa2015/serie_2001_2015_tcu.shtm
24. SESACRE, “Boletim semanal sala de comando e controle para combate a Dengue, Chikungunya e Zika ” (2016). http://www.agencia.ac.gov.br/wp-content/uploads/2016/04/BOLETIM-11-2016-final.pdf
25. Secretaria da Saúde do Estado de Bahia, “Situação epidemiológica das arboviroses. Bahia, 2016” (2016). http://www.suvisa.ba.gov.br/vigilancia_epidemiologica/consulta_boletim_epidemiologico/4427
26. Panamerican Health Organization, “Zika - Epidemiological Update 26 May 2016” (2016).

http://www.paho.org/hq/index.php?option=com_docman&task=doc_view&Itemid=270&gid=34797&lang=en

27. Secretaria da Saúde do Estado de Espírito Santo, “Boletim Epidemiológico – Dengue, Chikungunya e Zika ” (2016). http://mosquito.saude.es.gov.br/Media/dengue/Boletim%20Epidemiologico/Boletim%20Epid%20Dengue_01_2016_Final.pdf
28. L. Bastos *et al.*, Zika in Rio de Janeiro: Assessment of basic reproductive number and its comparison with dengue. *bioRxiv*, (2016).
29. Secretaria da Saúde do Estado de Estado de São Paulo, “Distribuição dos casos de Zika Vírus notificados e confirmados (autóctones e importados), segundo o município de residência por mês de início de sintomas. Estado de São Paulo, 2016” (2016). http://www.saude.sp.gov.br/resources/cve-centro-de-vigilancia-epidemiologica/areas-de-vigilancia/doencas-de-transmissao-por-vetores-e-zoonoses/dados/zika/zika16_dados.pdf
30. Secretaria da Saúde do Estado de Paraná, “Situação da Dengue, Chikungunya e Zika vírus no Paraná - 2015/2016” (2016). http://www.dengue.pr.gov.br/modules/conteudo/conteudo.php?conteudo=3
31. Secretaria da Saúde do Estado de Rio Grande do Sul, “Informativo Epidemiológico Dengue, Chicungunya, Zika Virus e Microcefalia ” (2016). http://ptdocz.com/doc/1623031/memorando-n%C2%BA---secretaria-estadual-da-sa%C3%BAde-do-rio-grande..
32. Secretaria da Saúde do Goiânia, “Informe Técnico Semanal: Dengue, Chikungunya, Zika E Microcefalia Relacionada À Infecção Congênita ” (2016). http://www.saude.goiania.go.gov.br/docs/divulgacao/Informe%20Semanal%20Den,_Chik,_Zika,_Micro_04_05_1_SE_17.pdf
33. Secretaria da Saúde do Estado de Mato Grosso, “Informes de Dengue, Chikungunya e Zika” (2016). http://www.saude.mt.gov.br/dengue/arquivos/526/documentos
34. Panamerican Health Organization, “Regional Zika Epidemiological Update (Americas) - 9 June 2016” (2016). http://www.paho.org/hq/index.php?option=com_docman&task=doc_view&Itemid=270&gid=34970&lang=en
35. Panamerican Health Organization, “Zika - Epidemiological Update 14 April 2016” (2016). http://www.paho.org/hq/index.php?option=com_docman&task=doc_view&Itemid=270&gid=34183&lang=en
36. Panamerican Health Organization, “Zika - Epidemiological Update 21 April 2016” (2016). http://www.paho.org/hq/index.php?option=com_docman&task=doc_view&Itemid=270&gid=34243&lang=en
37. O. Pacheco *et al.*, Zika Virus Disease in Colombia - Preliminary Report. *N Engl J Med*, [Epub ahead of print] (2016).
38. WHO, “Prevention of sexual transmission of Zika virus ” (2016). http://apps.who.int/iris/bitstream/10665/204421/1/WHO_ZIKV_MOC_16.1_eng.pdf?ua=1
39. O. Dyer, Jamaica advises women to avoid pregnancy as Zika virus approaches. *BMJ* **352**, (2016).
40. J. Daltón, “El Salvador recomienda evitar los embarazos hasta 2018 por el Zika,” *El País*, 2016.

http://internacional.elpais.com/internacional/2016/01/26/america/1453844344_353247.html

41. Acento Diario electrónico de la República Dominicana, "Ministra dominicana de Salud pide posponer embarazos este año por riesgo zika " (2016). http://acento.com.do/2016/actualidad/8317196-ministra-dominicana-de-salud-pide-posponer-embarazos-este-ano-por-riego-zika/
42. Ministerio de Salud y Protección Social de Colombia, "Circular 002, Enero 7, 2016" (2016). https://www.minsalud.gov.co/sites/rid/Lists/BibliotecaDigital/RIDE/DE/DIJ/Circular-02-de-2016.pdf
43. L. Barzon *et al.*, Isolation of infectious Zika virus from saliva and prolonged viral RNA shedding in a traveller returning from the Dominican Republic to Italy, January 2016. *Euro Surveill* **21**, (2016).
44. M. Besnard, S. Lastere, A. Teissier, V. Cao-Lormeau, D. Musso, Evidence of perinatal transmission of Zika virus, French Polynesia, December 2013 and February 2014. *Euro Surveill* **19**, (2014).
45. S. L. Robert *et al.*, Genetic and Serologic Properties of Zika Virus Associated with an Epidemic, Yap State, Micronesia, 2007. *Emerging Infectious Disease journal* **14**, 1232 (2008).
46. J. M. Mansuy *et al.*, Zika virus: high infectious viral load in semen, a new sexually transmitted pathogen?
47. A. Waehre T Fau - Maagard, D. Maagard A Fau - Tappe, D. Tappe D Fau - Cadar, J. Cadar D Fau - Schmidt-Chanasit, J. Schmidt-Chanasit, Zika virus infection after travel to Tahiti, December 2013.
48. L. Zammarchi *et al.*, Zika virus infections imported to Italy: clinical, immunological and virological findings, and public health implications. *J Clin Virol* **63**, 32-35 (2015).
49. G. Ann-Claire, O. C. Olivia, C. Elodie, G. Cyrille, D.-R. Myrielle, Detection of Zika Virus in Urine. *Emerging Infectious Disease journal* **21**, 84 (2015).
50. H. E. Clapham, V. Tricou, N. Van Vinh Chau, C. P. Simmons, N. M. Ferguson, Within-host viral dynamics of dengue serotype 1 infection. *J R Soc Interface* **11**, (2014).
51. H. E. Clapham *et al.*, Modelling Virus and Antibody Dynamics during Dengue Virus Infection Suggests a Role for Antibody in Virus Clearance. *PLoS Comput Biol* **12**, e1004951 (2016).
52. J. Lessler *et al.*, Times to Key Events in the Course of Zika Infection and their Implications for Surveillance: A Systematic Review and Pooled Analysis. *bioRxiv*, (2016).
53. M. N. Nguyet *et al.*, Host and viral features of human dengue cases shape the population of infected and infectious Aedes aegypti mosquitoes. *Proc Natl Acad Sci U S A* **110**, 9072-9077 (2013).
54. J. P. Boorman, J. S. Porterfield, A simple technique for infection of mosquitoes with viruses; transmission of Zika virus. *Trans R Soc Trop Med Hyg* **50**, 238-242 (1956).
55. M. Cornet, Y. Robin, C. Adam, M. Valade, M. A. Calvo, Transmission expérimentale comparée du virus amaril et du virus Zika chez Aedes aegypti L. Comparison between experimental transmission of Yellow fever and Zika viruses in Aedes aegypti. *Cahiers ORSTOM. Sér. Ent. Méd et Parasitol* **XVII**, 47-53. (In French.) (1979).
56. M. I. Li, P. S. Wong, L. C. Ng, C. H. Tan, Oral susceptibility of Singapore Aedes (Stegomyia) aegypti (Linnaeus) to Zika virus. *PLoS Negl Trop Dis* **6**, e1792 (2012).

57. P. S. Wong, M. Z. Li, C. S. Chong, L. C. Ng, C. H. Tan, Aedes (Stegomyia) albopictus (Skuse): a potential vector of Zika virus in Singapore. *PLoS Negl Trop Dis* **7**, e2348 (2013).

58. J. P. Ledermann *et al.*, Aedes hensilli as a potential vector of Chikungunya and Zika viruses. *PLoS Negl Trop Dis* **8**, e3188 (2014).

59. C. T. Diagne *et al.*, Potential of selected Senegalese Aedes spp. mosquitoes (Diptera: Culicidae) to transmit Zika virus. *BMC Infect Dis* **15**, 492 (2015).

60. R. Maciel-de-Freitas, C. T. Codeco, R. Lourenco-de-Oliveira, Daily survival rates and dispersal of Aedes aegypti females in Rio de Janeiro, Brazil. *Am J Trop Med Hyg* **76**, 659-665 (2007).

61. M. R. David, R. Lourenco-de-Oliveira, R. M. Freitas, Container productivity, daily survival rates and dispersal of Aedes aegypti mosquitoes in a high income dengue epidemic neighbourhood of Rio de Janeiro: presumed influence of differential urban structure on mosquito biology. *Mem Inst Oswaldo Cruz* **104**, 927-932 (2009).

62. A. Cori, N. M. Ferguson, C. Fraser, S. Cauchemez, A new framework and software to estimate time-varying reproduction numbers during epidemics. *Am J Epidemiol* **178**, 1505-1512 (2013).

63. M. Turelli, Cytoplasmic incompatibility in populations with overlapping generations. *Evolution* **64**, 232-241 (2010).

64. M. Otero, H. G. Solari, N. Schweigmann, A stochastic population dynamics model for Aedes aegypti: formulation and application to a city with temperate climate. *Bull Math Biol* **68**, 1945-1974 (2006).

65. P. M. Sheppard, W. W. Macdonald, R. J. Tonn, B. Grab, The Dynamics of an Adult Population of Aedes aegypti in Relation to Dengue Haemorrhagic Fever in Bangkok. *J Anim Ecol* **38**, 661-702 (1969).

66. T. W. Scott *et al.*, Longitudinal studies of Aedes aegypti (Diptera: Culicidae) in Thailand and Puerto Rico: blood feeding frequency. *J Med Entomol* **37**, 89-101 (2000).

67. L. M. Bartley, C. A. Donnelly, G. P. Garnett, The seasonal pattern of dengue in endemic areas: mathematical models of mechanisms. *Trans R Soc Trop Med Hyg* **96**, 387-397 (2002).

68. H. Nishiura, Mathematical and Statistical Analyses of the Spread of Dengue. *Dengue Bulletin* **30**, (2006).

69. V.-M. Cao-Lormeau *et al.*, Guillain-Barré Syndrome outbreak associated with Zika virus infection in French Polynesia: a case-control study. *The Lancet* **387**, 1531-1539 (2016).